Universality and self-similarity of an energy-constrained sandpile model with random neighbors

Shu-dong Zhang *
Institute of Low Energy Nuclear Physics, Beijing Normal University, Beijing 100875, China;
CCAST(World Laboratory), P.O. Box 8730, Beijing 100080, China;
Beijing Radiation Center, Beijing 100088, China;
and Institute of Theoretical Physics, Beijing Normal University, Beijing 100875, China
(Received 25 January 1999)

We study an energy-constrained sandpile model with random neighbors. The critical behavior of the model is in the same universality class as the mean-field self-organized criticality sandpile. The critical energy E_c depends on the number of neighbors n for each site, but the various exponents are independent of n. A self-similar structure with $n-1$ major peaks is developed for the energy distribution $p(E)$ when the system approaches its stationary state. The avalanche dynamics contributes to the major peaks appearing at $E_{p_k}=2k/(2n-1)$ with $k=1,2,\ldots,n-1$, while the fine self-similar structure is a natural result of the way the system is disturbed. [S1063-651X(99)10307-6]

PACS number(s): 05.65.+b, 05.40.−a, 05.70.Ln, 45.05.+x

I. INTRODUCTION

According to the original work of Bak *et al.* on self-organized criticality [1], driven dissipative systems with many coupled degrees of freedom would evolve spontaneously into a critical state without fine tuning any control parameter. The critical state of such a system is characterized by scale-free distributions of dynamical activities. Bak *et al.* demonstrated their idea with a cellular automaton model, the Bak-Tang-Wiesenfeld (BTW) sandpile model, which later on drew much attention from physicists. Several variations [2–4] of the BTW model and some other models, such as the forest-fire model [5], the spring-block model [6], the Bak-Sneppen model [7], etc., were proposed and were shown to display self-organized criticality (SOC) behaviors. There have also been many efforts [8,9] to identify the mechanism that leads to scale-free distributions in SOC models. For sandpile models, scale invariance can be shown to follow from a local conservation law [10], while in the nonconservative stick-slip model [6] the synchronization of system elements plays an important role [9]. As yet there seems to be no unified picture for the appearance of SOC behavior.

To many physicists, the idea of a critical point without fine tuning of external parameters is very appealing because it opposes the standard picture of the equilibrium critical phenomenon. Recently, several authors [11,12] argued that in SOC systems the driving rate actually acts as the control parameter that has to be fine-tuned to zero to observe criticality. For instance, the SOC models usually involve a separation of time scales, namely, the slow time scale of driving and the fast (instant) time scale of relaxation (avalanche). So SOC models are actually defined at the driving rate of zero. To shed more light on the properties of SOC models, a sandpile model with constrained total energy was proposed [13]. The energy-constrained (EC) sandpile model differs from the SOC sandpile model in the following way. In the SOC model there are both input of energy into the system and dissipation of energy from the boundary. When the stationary state of the system is reached, the input and the dissipation balance each other statistically, nevertheless there is still fluctuation of the total energy. In the EC model, however, there is neither input nor dissipation of system energy, and the dynamics just redistributes energy among system elements. So the total energy is fixed and thus is a control parameter. Numerical studies of the EC sandpile revealed that the model exhibits power-law distribution of avalanche sizes at the critical energy $E_c=(0.6492\pm0.0002)E_{\rm th}$ [13], with the same exponents as that of the corresponding SOC sandpile. The scaling with the distance to the critical point, however, is different from that of the SOC model. For the EC sandpile, $\langle s\rangle \sim(E_c-\overline{E})^{-\gamma}$ with $\gamma=1.41\pm0.03$, while for the SOC sandpile $\gamma=1$. The authors of Ref. [13] concluded that the EC sandpile and the corresponding SOC sandpile were in different universality classes. This result, as stated in Ref. [13], appears somewhat puzzling. A natural question to ask is, are EC models necessarily in different universality classes from their corresponding SOC models?

II. RANDOM NEIGHBOR EC SANDPILE MODEL

In this paper, we will study a continuous-energy sandpile model with random neighbors (RN) and constrained total energy. A continuous-energy SOC model defined on a square lattice with stochastic driving was first introduced in Ref. [14], and the critical energy was measured to be $E_c=(0.62\pm0.01)E_{\rm th}$. Here we consider a system with a total number N of sites. To each of them a continuous non-negative variable, say *energy*, is associated. If the energy E_i of site i is less than some threshold value $E_{\rm th}$, the site i is said to be stable. By properly choosing units, we can set $E_{\rm th}=1$. If $E_i\geqslant1$, the site is unstable and will release all its energy. The energy E_i of this unstable site will be evenly divided into n portions, where the integer $n>1$ will be referred to as the number of neighbors for each site. These portions of energy will be at first temporally put into an energy ''*buffer*,'' and then will be given back to system sites one by one. Each portion of energy will be given to a randomly chosen site,

*Electronic address: zhangsd@bnu.edu.cn

 ©1999 The American Physical Society

say site j, from the system. So the energy of site j becomes $E_j \rightarrow E_j + E_i/n$. If site j also becomes unstable by receiving a portion of energy, it will also release all its energy E_j which in turn will be divided and put into the buffer. The energy portions in the buffer follow a ''first in first out'' rule, and the process continues until the energy buffer becomes empty. The successive energy releasing of unstable sites will be called an *avalanche*, and the size s of an avalanche is defined as the total number of releasing sites during the avalanche. In this model, system sites are randomly chosen to receive energy portions from the buffer, and it is in this sense that the model is called a random-neighbor model.

When an avalanche has stopped, the system becomes stable; we disturb the system by randomly choosing a site, dividing its energy evenly into n portions and putting the energy portions into the buffer. Note that the way we disturb the system is different from the ways employed in Ref. [13], namely, the random subtraction (RS) and the continuous subtraction (CS). We will see later that the disturbance we employed here will generate a self-similar structure in the energy distribution.

In the present model, the avalanche dynamics and the disturbance both conserve the total energy of the system, so the total energy never changes, and it is in this sense the model is energy-constrained. We will use $N\overline{E}$ to denote the total energy of the system, so the average energy per site is $\overline{E}$. For brevity we just call $\overline{E}$ the system energy. We will study the critical behavior of the model as the value of $\overline{E}$ is continuously tuned.

III. DETERMINATION OF THE CRITICAL ENERGY

The critical energy E_c is the system energy at which the system has a scale-free distribution of avalanche sizes. In other words, at the critical energy there is no characteristic avalanche size, and the size distribution is expected to be a power law. Let us define the quantity $\epsilon = E_c - \overline{E}$ as the distance from the critical point. At the critical point $\epsilon = 0$ one has a pure power-law distribution $P(s) \sim s^{-\tau}$. Near the critical point, a cutoff size, $s_c \sim \epsilon^{-1/\sigma}$, is expected to be present due to the departure from the critical point. In numerical simulations, one can only study systems of finite size N. Due to the finite-size effect, one expects a saturation of s_c when $\epsilon \rightarrow 0$, in the form $s_c \sim \epsilon^{-1/\sigma} f(\epsilon/N^{-\rho})$, and finally one has the following form of avalanche distribution:

$$P(s,\epsilon,N) = s^{-\tau} G\left(\frac{s}{\epsilon^{-1/\sigma} f(\epsilon/N^{-\rho})} \right). \tag{1}$$

Here two scaling functions $G(x)$ and $f(x)$ are introduced. $G(x)$ is a constant for $x<1$ and drops down rapidly for $x>1$; $f(x)$ is a constant for large enough x, and follows a power law $f(x) \sim x^{1/\sigma}$ for $x \ll 1$. In the following sections we will verify Eq. (1) with numerical results from different aspects, and will determine the exponents τ, σ, and ρ.

We determine the critical energy E_c by identifying a good power-law behavior of $\langle s \rangle$ with N. In Fig. 1, we show $\langle s \rangle$ as a function of N for different values of $\overline{E}$. When $\overline{E}$ is small, $\langle s \rangle$ increases with N slower than a power law and eventually it saturates to some constant. For large $\overline{E}$, $\langle s \rangle$ increases with

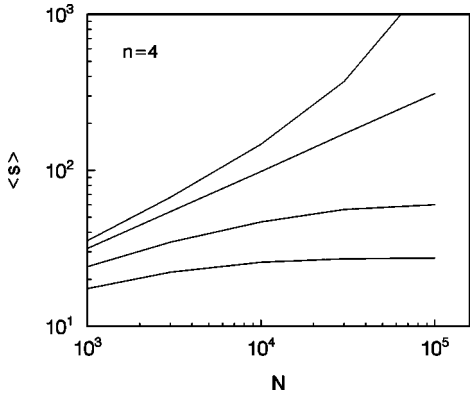

FIG. 1. Average size of avalanches for different system energy $\overline{E}$. The curves (from top to bottom) are for $\overline{E} = 0.43, 0.4286, 0.425$, and 0.42, respectively. Note that the curve for $\overline{E} = 0.4286$ can be fitted to a power law $\langle s \rangle \sim N^{d_f}$ very well with $d_f = 0.50 \pm 0.01$.

N faster than a power law and will never saturate. There is a value E_c at which $\langle s \rangle$ has a very good power-law dependence on N, $\langle s \rangle \sim N^{d_f}$, and this is just the critical energy of the system. By the procedure described above, we get that $E_c = 0.4286 \pm 0.0001$ and $d_f = 0.50 \pm 0.01$ for $n = 4$. Note that this critical energy is different from that of the EC sandpile defined on a square lattice, where $E_c = (0.6492 \pm 0.0002) E_{\text{th}}$ [13]. For $n = 6$, we get $E_c = 0.4545 \pm 0.0001$ and $d_f = 0.50 \pm 0.01$. The numerical results suggest that the critical energy is dependent on n, but the exponent d_f is independent of n.

IV. AVALANCHE-SIZE DISTRIBUTION AT THE CRITICAL POINT

As expected from the above discussions, the avalanche-size distribution follows a power law at the critical energy E_c. For finite N the numerical results can be well described by the following form:

$$P(s,N) = s^{-\tau} G(s/N^D). \tag{2}$$

The scaling function $G(x)$ is a constant when $x<1$ and drops rapidly for $x>1$. In fact, Eq. (2) can be obtained from Eq. (1) by taking the limit $\epsilon \rightarrow 0$ with $D = \rho/\sigma$.

In Fig. 2, we show the avalanche-size distribution at the critical energy. By a data-collapse technique, we determined

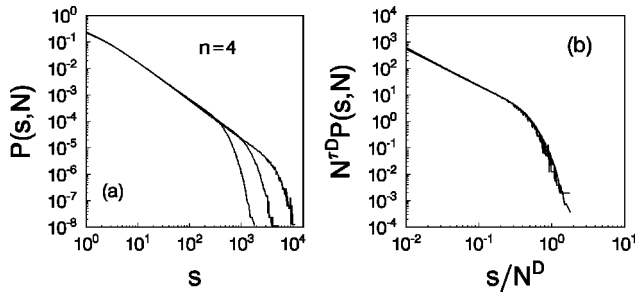

FIG. 2. (a) Avalanche size distribution for $n = 4$ at the critical point $\overline{E} = 0.4286$. The curves (from right to left) are for $N = 10\,000, 3000$, and 1000, respectively. The statistics were made over 10^8 avalanches. (b) A data collapse according to Eq. (2), with the exponents $\tau = 1.5$ and $D = 1$.

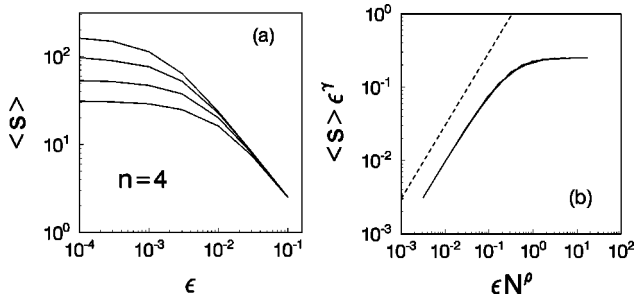

FIG. 3. (a) Average size of avalanches scales with $\epsilon = E_c - \overline{E}$ for different N. The curves (from top to bottom) are for $N = 30\,000, 10\,000, 3000$, and 1000, respectively. (b) Data collapse according to Eq. (5), with the exponents $\gamma = 1$ and $\rho = 0.5$. The dashed line shows a curve $y \propto x^{\gamma}$ for reference.

the exponents $\tau = 1.50 \pm 0.02$ and $D = 1.0 \pm 0.1$. One can also get a scaling relation between τ, D, and d_f by

$$\langle s \rangle(N) = \int sP(s,N)ds \sim \int s^{1-\tau} G(s/N^D)ds \propto N^{D(2-\tau)}. \tag{3}$$

So one has that $d_f = D(2-\tau)$. The numerical results for D, τ, and d_f agree well with this scaling relation. Again we find that exponents D, τ, and d_f for $n = 6$ are the same as for $n = 4$ within numerical errors.

The avalanche exponent τ here is the same as the mean-field result for various SOC models [12,15]. In the present model, the avalanche can be actually mapped to a random walk problem [15] or to a branching process [16]. In both cases, the corresponding exponent can be shown to be 1.5. At the critical point, the branching rate is equal to unity. For the present model, the branching rate can be calculated by

$$r_b = n \int_{1-\langle E^+ \rangle / n}^{1} p(E)dE, \tag{4}$$

where $p(E)$ is the energy distribution function and $\langle E^+ \rangle$ is the average releasing energy of unstable sites. We have made some calculations on r_b. At the critical energy E_c, we did get that $r_b = 1$ within numerical errors. This verifies that the critical energy was consistently determined.

V. SCALING WITH THE DISTANCE TO THE CRITICAL POINT

To see if the EC model is in the same universality class as its SOC counterpart, one needs to investigate the scaling with the distance to the critical point. Calculating the average size of avalanches by using Eq. (1), one gets the following scaling form:

$$\langle s \rangle \sim \epsilon^{-\gamma} F\left(\frac{\epsilon}{N^{-\rho}} \right), \tag{5}$$

with $\gamma = (2-\tau)/\sigma$ and $F(x) = f^{2-\tau}(x)$, which is the $(2-\tau)$th power of $f(x)$. $F(x)$ follows a power law $F(x) \sim x^{\gamma}$ for $x \ll 1$ and becomes constant for $x \gg 1$. In Fig. 3 we show $\langle s \rangle$ as a function of $\epsilon = E_c - E$ for different N. A very good data collapse according to Eq. (5) is also obtained. The exponents extracted from the data collapse are $\gamma = 1.0$ and $\rho = 0.5$. So one has $\sigma = (2-\tau)/\gamma = 0.5$. Note that the relation $D = \rho/\sigma$ is consistently satisfied by the numerical results.

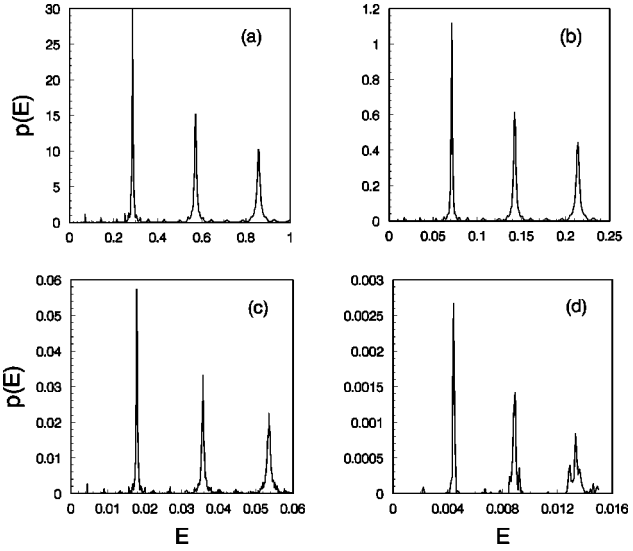

FIG. 4. The energy distribution for the case $n = 4$, $\overline{E} = 0.4286$. The statistics were made over 10^6 avalanches and the bin size is set to be 10^{-4}. To see the self-similar structure, parts of the figure were enlarged successively, (a)→(b)→(c)→(d).

One can also get that $\langle s \rangle \propto N^{\rho\gamma}$ by taking the limit $\epsilon \to 0$ in Eq. (5), and get the relation $d_f = \rho\gamma$. The numerical results also agree well with this relation. Also note that the exponents γ and ρ for $n = 6$ are the same as that for $n = 4$ although the critical energies are different for the two cases.

So, for the EC RN sandpile model, not only the avalanche exponent $\tau = 1.5$ but also the scaling exponent $\gamma = 1$ is the same as that of the mean-field SOC model. This situation is different from the case studied in Ref. [13], where the exponent γ for the EC model is different from that of the SOC model.

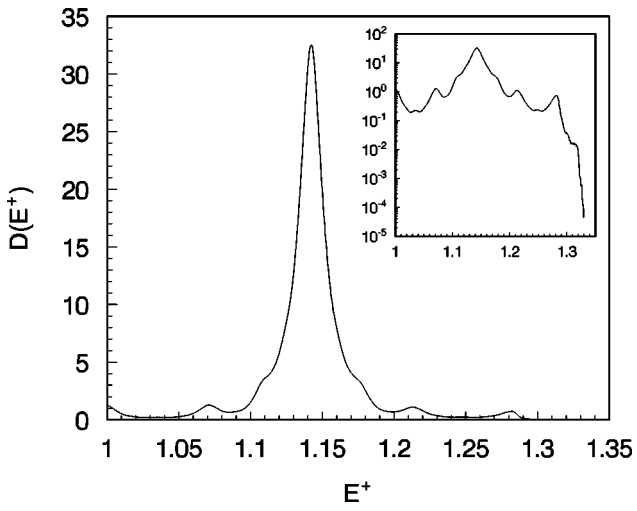

FIG. 5. The releasing energy distribution for the case $n = 4$, $\overline{E} = 0.4286$. The statistics were made over 8×10^7 unstable releasing events and the bin size is set to be 5×10^{-4}. The pronounced peak in the figure is at $E_m^+ = 1.1425$. The inset is the same curve replotted with $D(E^+)$ in logarithmic scale, which shows that the range of E^+ does not exceed the upper bound $n/(n-1) = 4/3 \approx 1.33$.

TABLE I. The most probable releasing energy E_m^+ and the positions of the major peaks E_{p_k}'s in the energy distribution $p(E)$. For each n the first line gives the numerical results, while the numbers in parentheses are calculated by $E_m^+=2n/(2n-1)$ and $E_{p_k}=kE_m^+/n=2k/(2n-1)$ with integer $k=1,2,3,\ldots,n-1$.

n	E_m^+	E_{p_1}	E_{p_2}	E_{p_3}	E_{p_4}	E_{p_5}
4	1.143 ± 0.001	0.285 ± 0.001	0.571 ± 0.001	0.86 ± 0.01	No	No
	(1.142857)	(0.285714)	(0.571429)	(0.857143)	No	No
5	1.11 ± 0.01	0.22 ± 0.01	0.44 ± 0.01	0.67 ± 0.01	0.89 ± 0.01	No
	(1.111111)	(0.222222)	(0.444444)	(0.666667)	(0.888889)	No
6	1.090 ± 0.001	0.181 ± 0.001	0.363 ± 0.001	0.545 ± 0.001	0.727 ± 0.001	0.91 ± 0.01
	(1.090909)	(0.181818)	(0.363636)	(0.545455)	(0.727273)	(0.909091)

VI. ENERGY DISTRIBUTION AT THE CRITICAL POINT

In this section we study the energy distribution of the system in its critical stationary state. Let $p(E)dE$ be the probability that a site has energy in the interval $[E,E+dE]$. In numerical simulations, we start from random energy configurations with a uniform distribution $p(E)=1/(2\overline{E})$, $0<E<2\overline{E}$, and let the system evolve according to the avalanche dynamics and disturbance. During the system evolution, avalanches distribute energies of unstable sites, and disturbances distribute energies of stable sites. Since disturbances and avalanches distribute energies in a similar way, it is expected to observe some type of self-similar structure in the energy distribution. We make statistics of $p(E)$ when the system approaches its stationary state. We find that $p(E)$ develops several major peaks. More interesting is the self-similar structure of $p(E)$. In Fig. 4, we show the energy distribution for the case $n=4$, $\overline{E}=0.4286$, and enlarge parts of the plot successively. A self-similar structure is obvious. Note that in Ref. [14], energy distribution with several peaks was also reported, but no self-similar structure of $p(E)$ was found there. In fact, the self-similar structure of $p(E)$ in the present model is a natural result of the avalanche dynamics and the way the system is disturbed. The avalanches (energy releasing of unstable sites) contribute to the major peaks, while the disturbances give rise to the fine self-similar structure. Clearly, there is an upper bound E_u^+ for the releasing energy, which should satisfy $E_u^+\leqslant 1+E_u^+/n$. So one has that $E_u^+\leqslant n/(n-1)$. Here we use a superscript plus to indicate releasing energy. Looking at the distribution $D(E^+)$ for the releasing energy (see Fig. 5, for example), one sees a pronounced peak at a value E_m^+, the most probable releasing energy. This means that most energy portions in the energy buffer have energy around E_m^+/n. These portions of energy, when successively given back to system sites, will give rise to the major peaks in $p(E)$. The positions of major peaks will be at $E_{p_k}=kE_m^+/n$, with integer $k=1,2,3,\ldots,n-1$. Since $E<1$ for stable sites, it is clear that k must be less than n, so that there are generally $n-1$ major peaks for $p(E)$. Given the $n-1$ major peaks in $p(E)$, the disturbances will produce smaller and smaller peaks in a similar way to how the avalanches produce the major peaks, hence the self-similar structure of $p(E)$ emerges. In principle, the self-similar behavior of $p(E)$ should go to infinitely small scale. Due to limited statistics and numerical resolution, however, we only show the self-similar structure with four levels in Fig. 4.

As the value of the most probable releasing energy E_m^+ is concerned, our numerical results suggest that $E_m^+=2n/(2n-1)$, but unfortunately proof of this result is still lacking. In Table I, we present some results for E_m^+ and E_{p_k}'s obtained from numerical simulations. The corresponding values calculated by $E_m^+=2n/(2n-1)$ and $E_{p_k}=kE_m^+/n$ are also given. One can see that they agree very well. Note that the self-similar structure of $p(E)$ is insensitive to the initial energy configurations. We have tried to start simulations from the initial distribution $p(E)=\delta(E-\overline{E})$, where $\overline{E}$ is the system energy, and found the same self-similar $p(E)$ when the system reached its critical stationary state.

VII. CONCLUSION

In conclusion, we have studied a random neighbor version of the EC sandpile model. The total energy of the system is a control parameter, which should be fine-tuned to observe criticality. The critical energy E_c depends on the number of neighbors n for each site, but the critical exponents are independent of n. This model is in the same universality class as the mean-field SOC sandpiles. The exponents $\tau=1.5$ and $\gamma=1$ are all the same as the mean-field results of SOC models. In this paper, we employed a special way to disturb the system when it is stable. The disturbance distributes stable energy ($E<1$) in a similar way to how the avalanche distributes unstable energy ($E^+\geqslant 1$). In its critical stationary state the model gives rise to a novel self-similar structure of the energy distribution, which is due to the particular way the system is disturbed.

ACKNOWLEDGMENTS

This work was supported by the National Nature Science Foundation of China, the Education Ministry of the State Council, through the Foundation of Doctoral Training.

[1] P. Bak, C. Tang, and K. Wiesenfeld, Phys. Rev. Lett. **59**, 381 (1987) Phys. Rev. A **38**, 364 (1988).
[2] L. Kadanoff, S. Nagel, L. Wu, and S. Zhou, Phys. Rev. A **39**, 6524 (1989).
[3] D. Dhar, Phys. Rev. Lett. **64**, 1613 (1990); D. Dhar and S. Majumdar, J. Phys. A **23**, 4333 (1990).
[4] S.S. Manna, J. Phys. A **24**, L363 (1991); P. Grassberger and S.S. Manna, J. Phys. (France) **51**, 1077 (1990).
[5] P. Bak, K. Chen, and C. Tang, Phys. Lett. A **147**, 297 (1990).
[6] Z. Olami, H.J.S. Feder, and K. Christensen, Phys. Rev. Lett. **68**, 1244 (1992); K. Christensen and Z. Olami, Phys. Rev. A **46**, 1829 (1992).
[7] P. Bak and K. Sneppen, Phys. Rev. Lett. **71**, 4083 (1993).
[8] G. Grinstein, D.-H. Lee, and S. Sachdev, Phys. Rev. Lett. **64**, 1927 (1990).
[9] A.A. Middleton and C. Tang, Phys. Rev. Lett. **74**, 742 (1995).
[10] S. Majumdar and D. Dhar, Physica A **185**, 129 (1992).
[11] D. Sornette, A. Johansen, and I. Dornic, J. Phys. I **5**, 325 (1995).
[12] A. Vespignani and S. Zapperi, Phys. Rev. Lett. **78**, 4793 (1997); Phys. Rev. E **57**, 6345 (1998).
[13] A. Chessa, E. Marinari, and A. Vespignani, Phys. Rev. Lett. **80**, 4217 (1998).
[14] Y.-C. Zhang, Phys. Rev. Lett. **63**, 470 (1989).
[15] H. Flyvbjerg, Phys. Rev. Lett. **76**, 940 (1996).
[16] T. E. Harris, *The Theory of Branching Processes* (Dover, New York, 1989).